

GNSS Reflectometry For Ionospheric Observation

African Capacity Building Workshop on Space Weather Effects on GNSS

Jade Morton

Satellite Navigation and Sensing Lab

University of Colorado Boulder

Jade.Morton@Colorado.edu

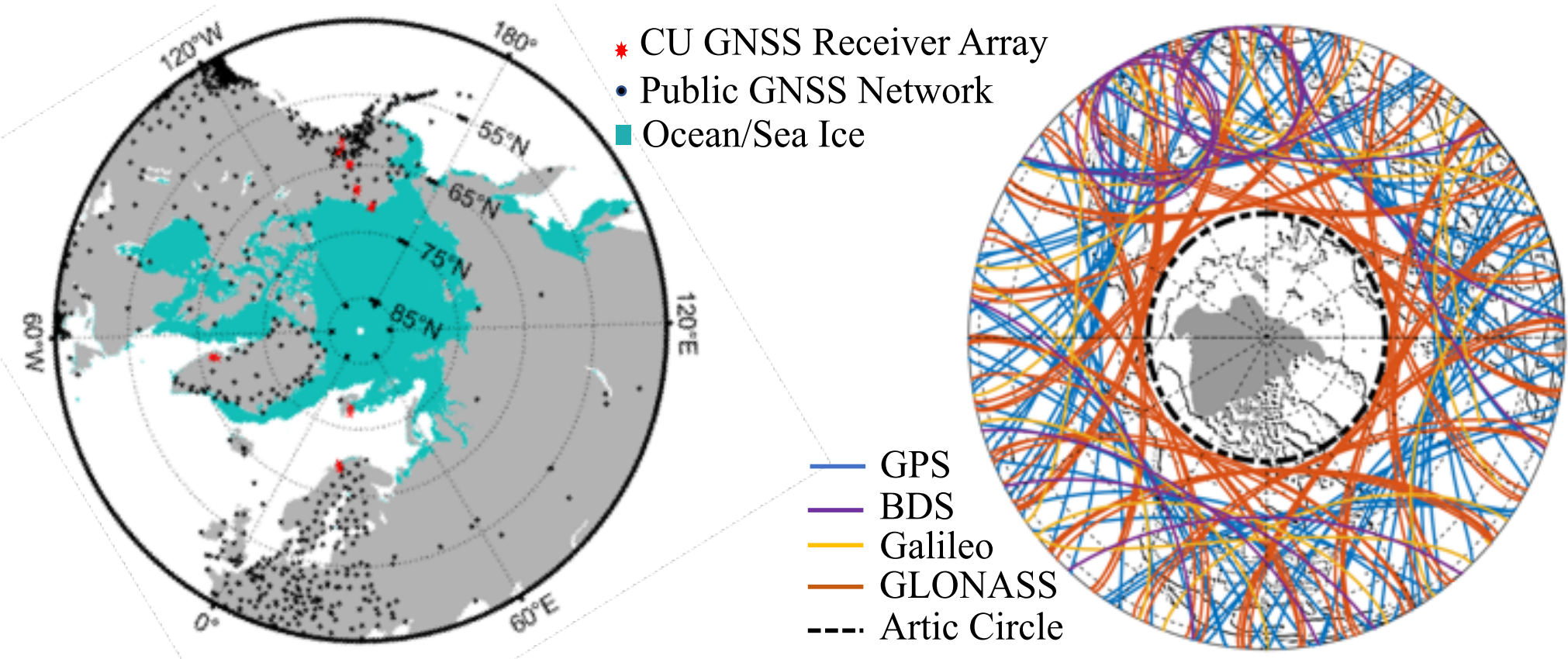


Outline

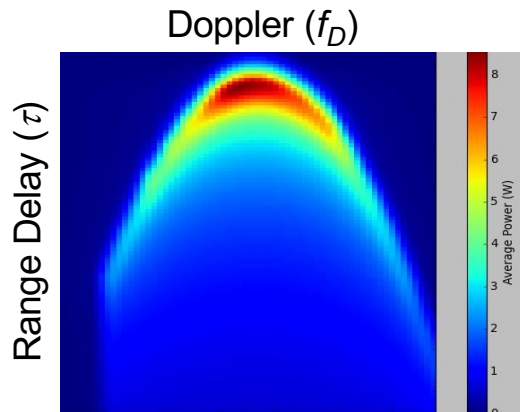
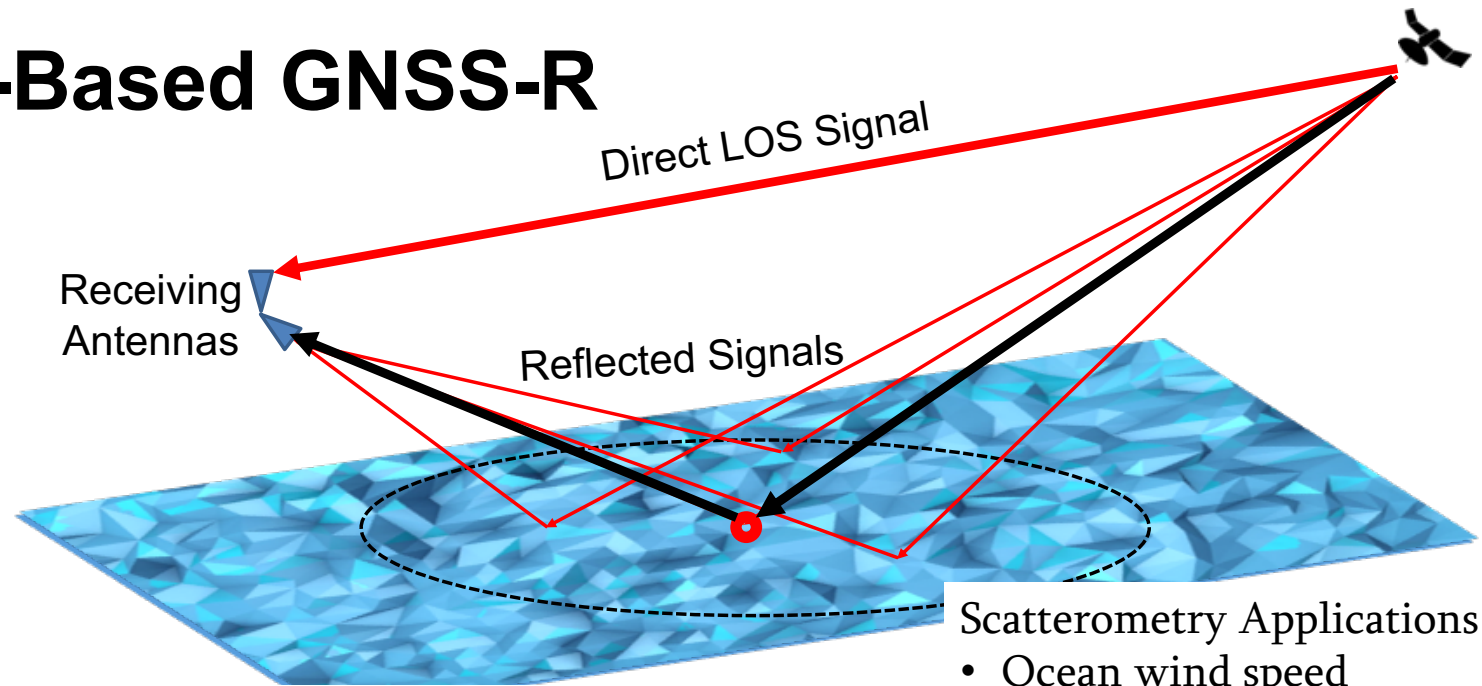
1. Background and Motivation
2. GNSS-R for Ionospheric Monitoring
3. Challenges and Opportunities



Data Gap Over Polar Regions

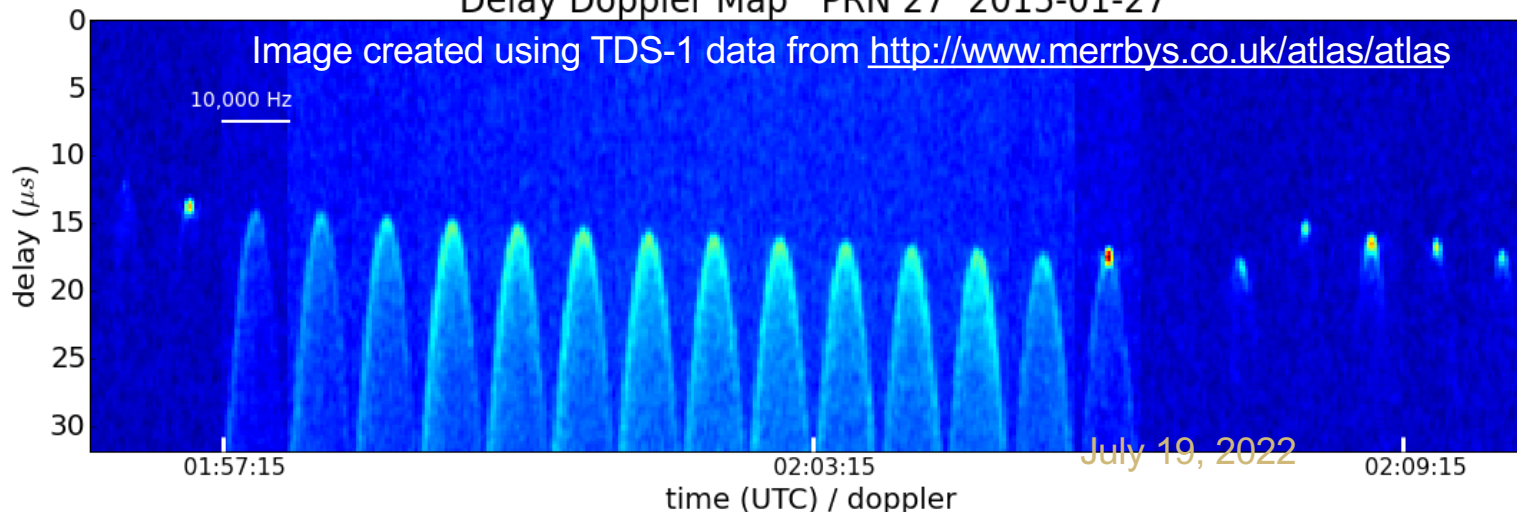


LEO Satellite-Based GNSS-R



Delay Doppler Map PRN 27 2015-01-27

Image created using TDS-1 data from <http://www.merrbys.co.uk/atlas/atlas>



Scatterometry Applications

- Ocean wind speed
- Land surface water content
- Soil moisture

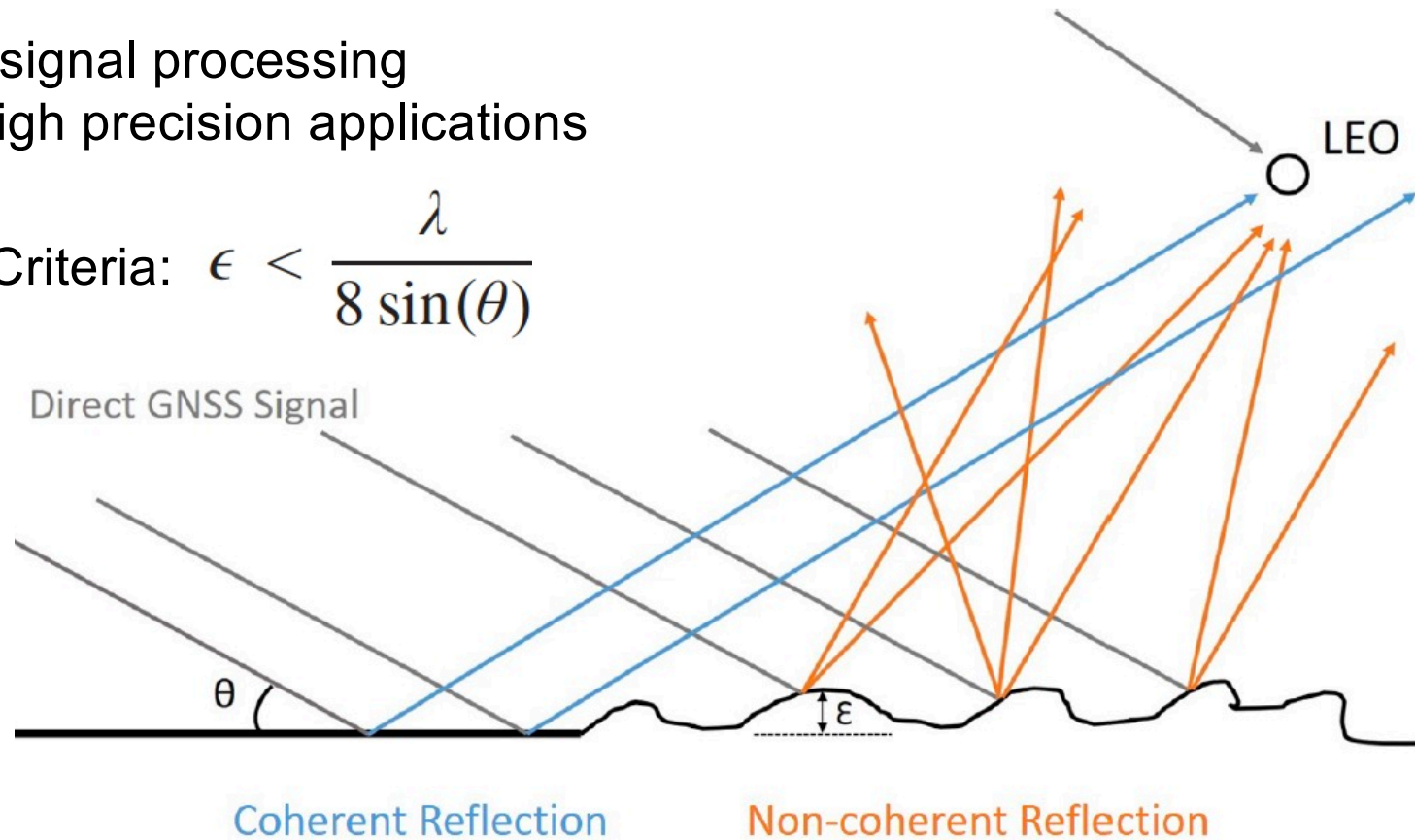
Altimetry Applications

- Sea surface height
- Sea ice topography
- Inland water body
- Ionosphere TEC, scintillation

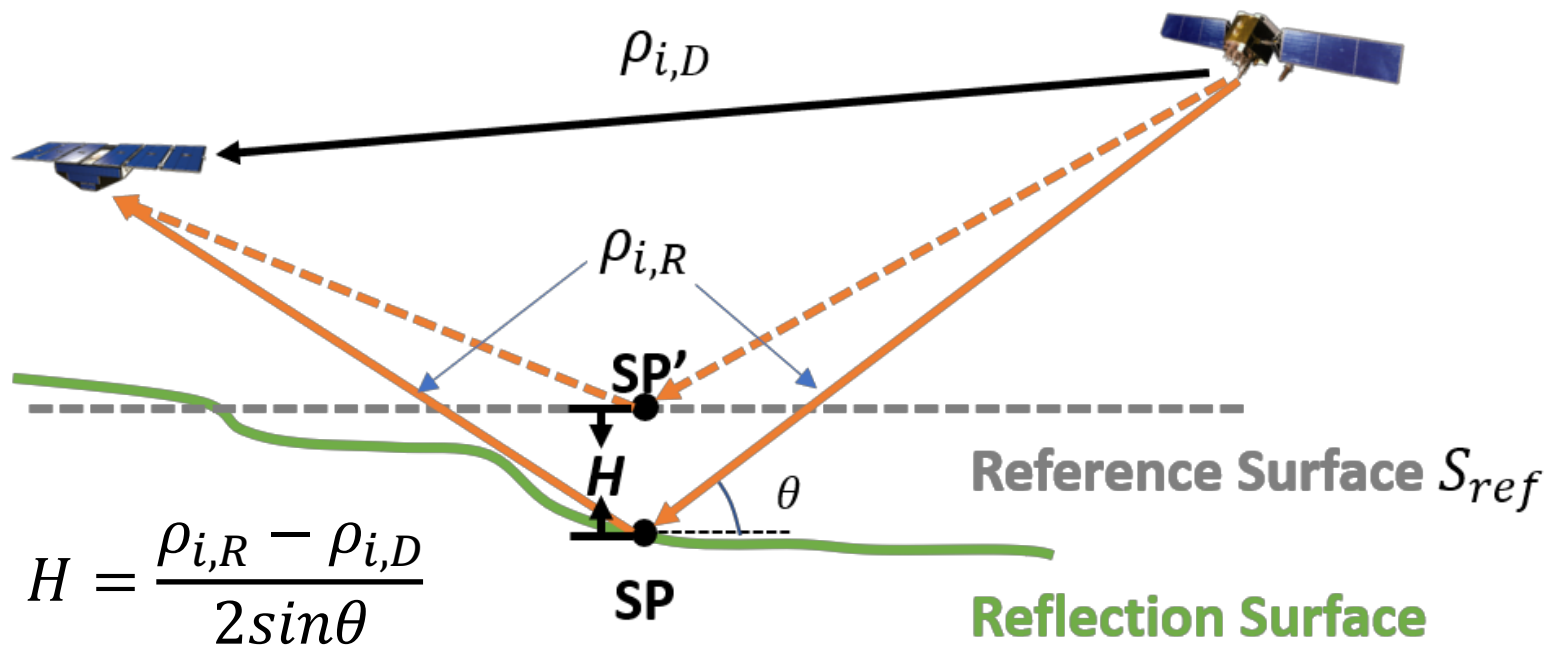
Coherent GNSS Reflections

Coherent signal processing
enables high precision applications

Rayleigh Criteria: $\epsilon < \frac{\lambda}{8 \sin(\theta)}$

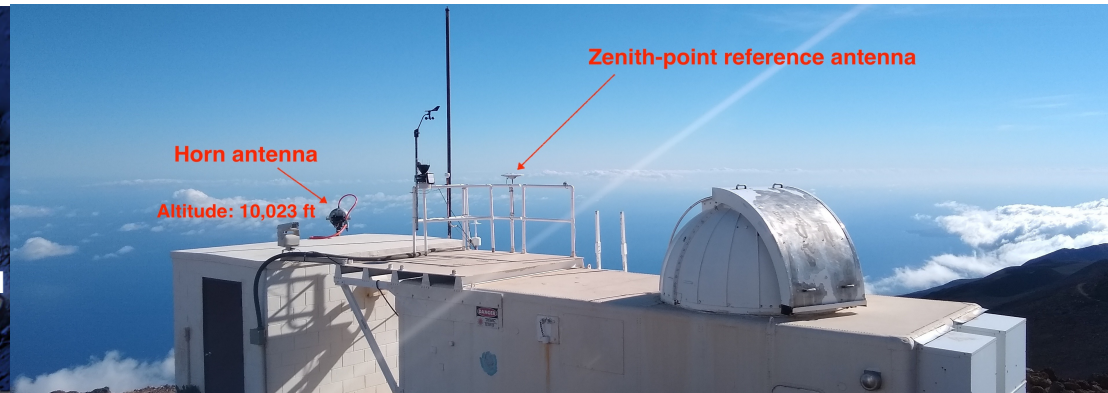
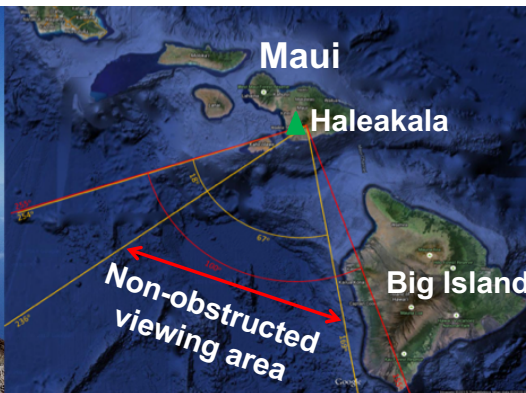
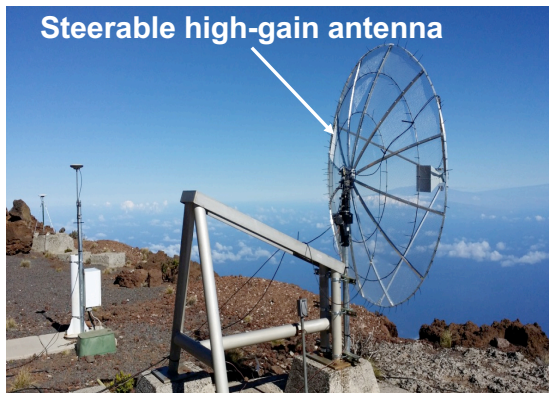
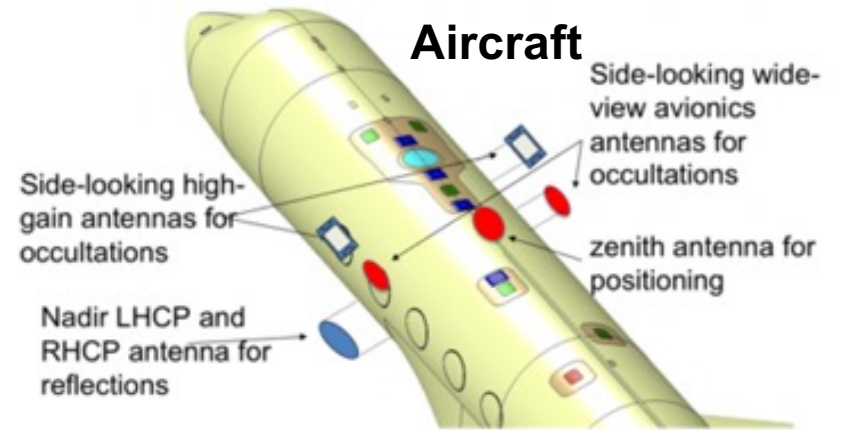
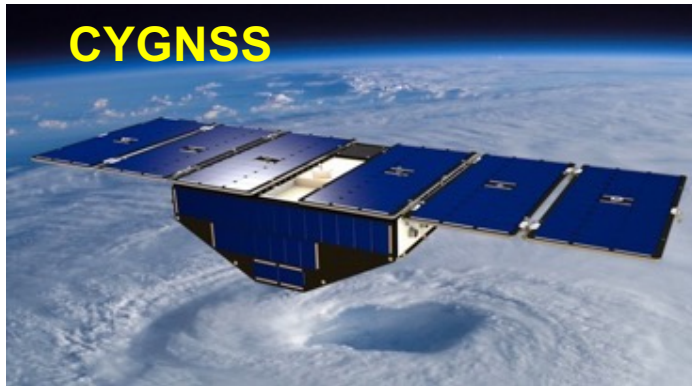


Space-borne GNSS-R Altimetry



Wang, Y., Y. Morton, "Coherent GNSS reflection signal processing for high-precision and high-resolution spaceborne applications," *IEEE Trans. Geosci. Remote Sensing*, DOI:10.1109/TGRS.2020.2993804, 2021.

GNSS-R Data Sources



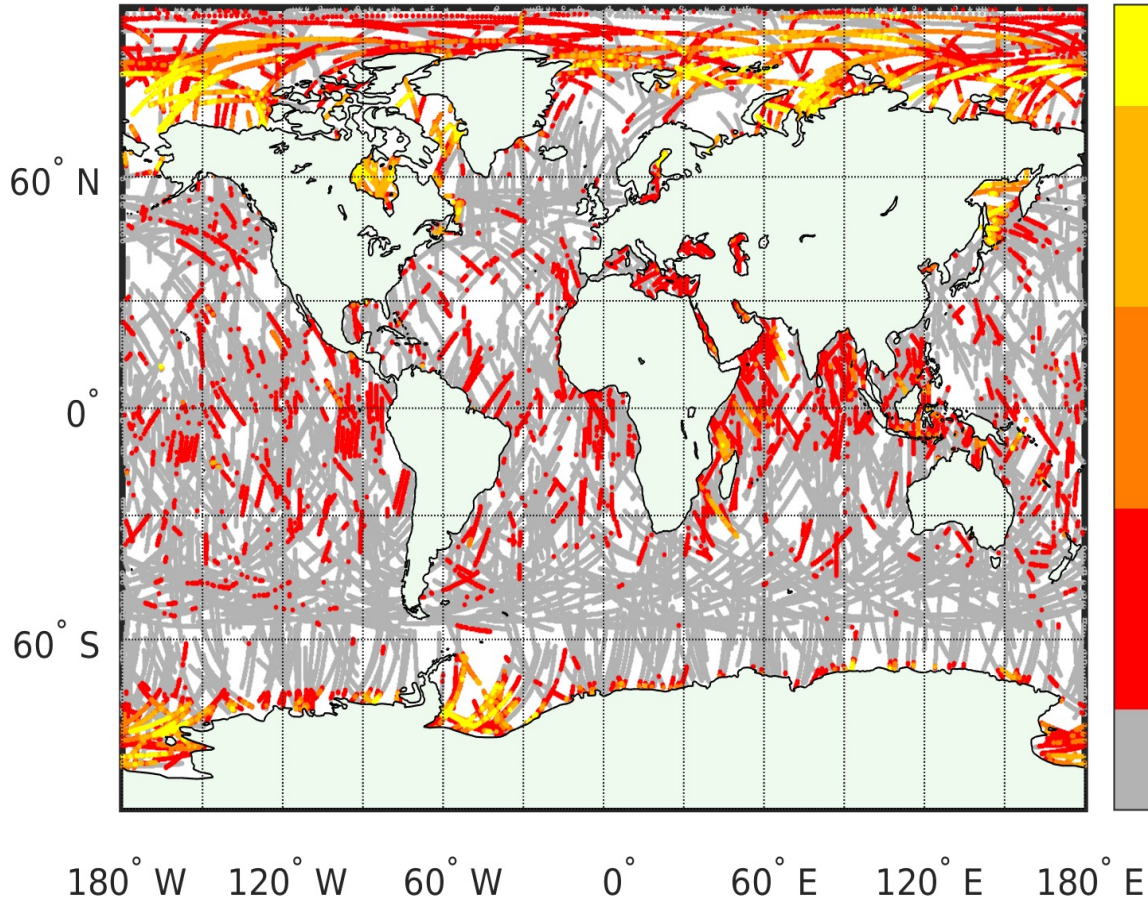
Coherent Reflection Statistics: Spire Global CubeSat

Surface type		% coherent reflections
Ocean	Global average	1%
	Wind speed < 5m/s	15%
	Within 200km of coast lines	5.5%
	Indonesia Archipelago	23%
Sea Ice	Global average	44.3%
	Multi-year ice	32%
	First year ice	75%

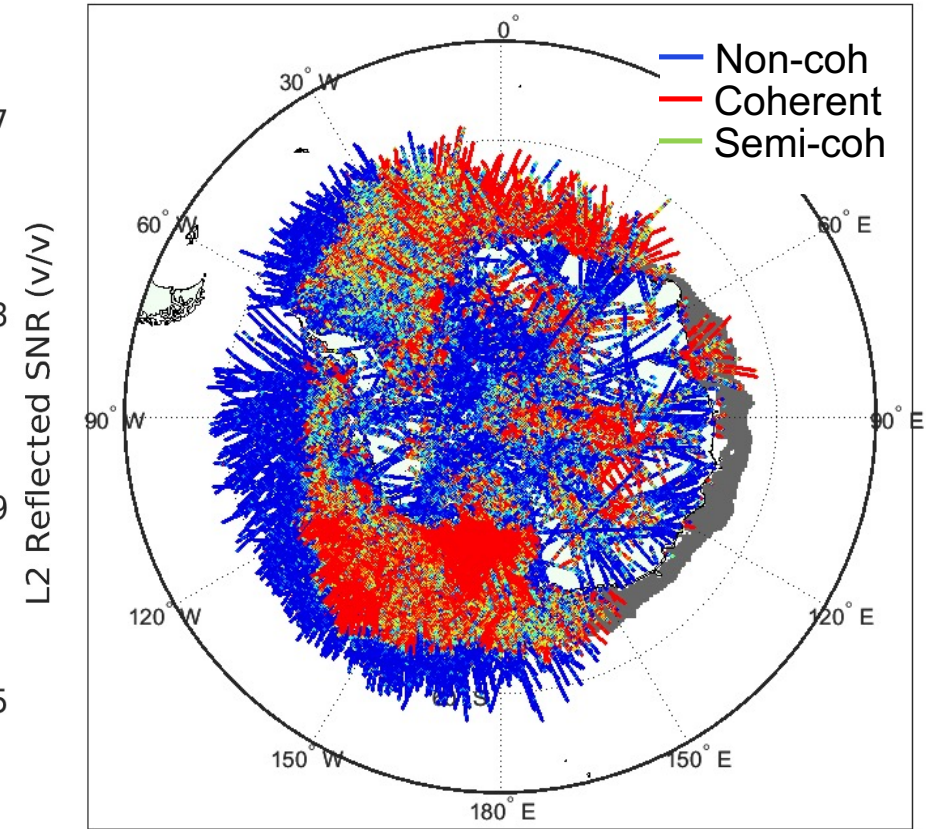
Roesler, C., Y. J. Morton, Y. Wang, R. S. Nerem, “Coherent GNSS-reflections characterization over ocean and sea ice based on Spire Global CubeSat data,” IEEE Trans. Geosci. Remote Sensing, DOI: 10.1109/TGRS.2021.3129999, 2021.



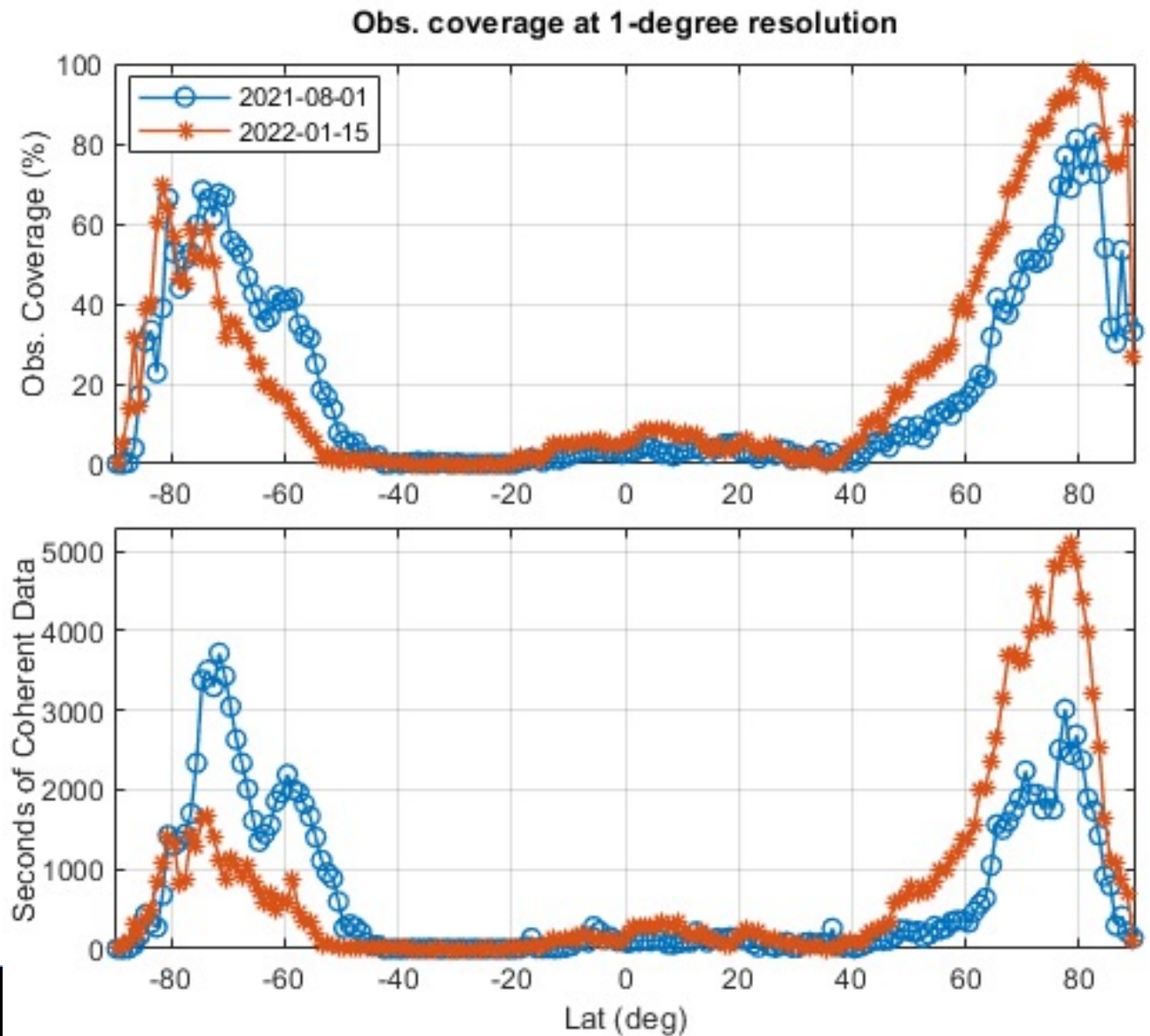
Spire GNSS-R Data: Jan-Apr 2019



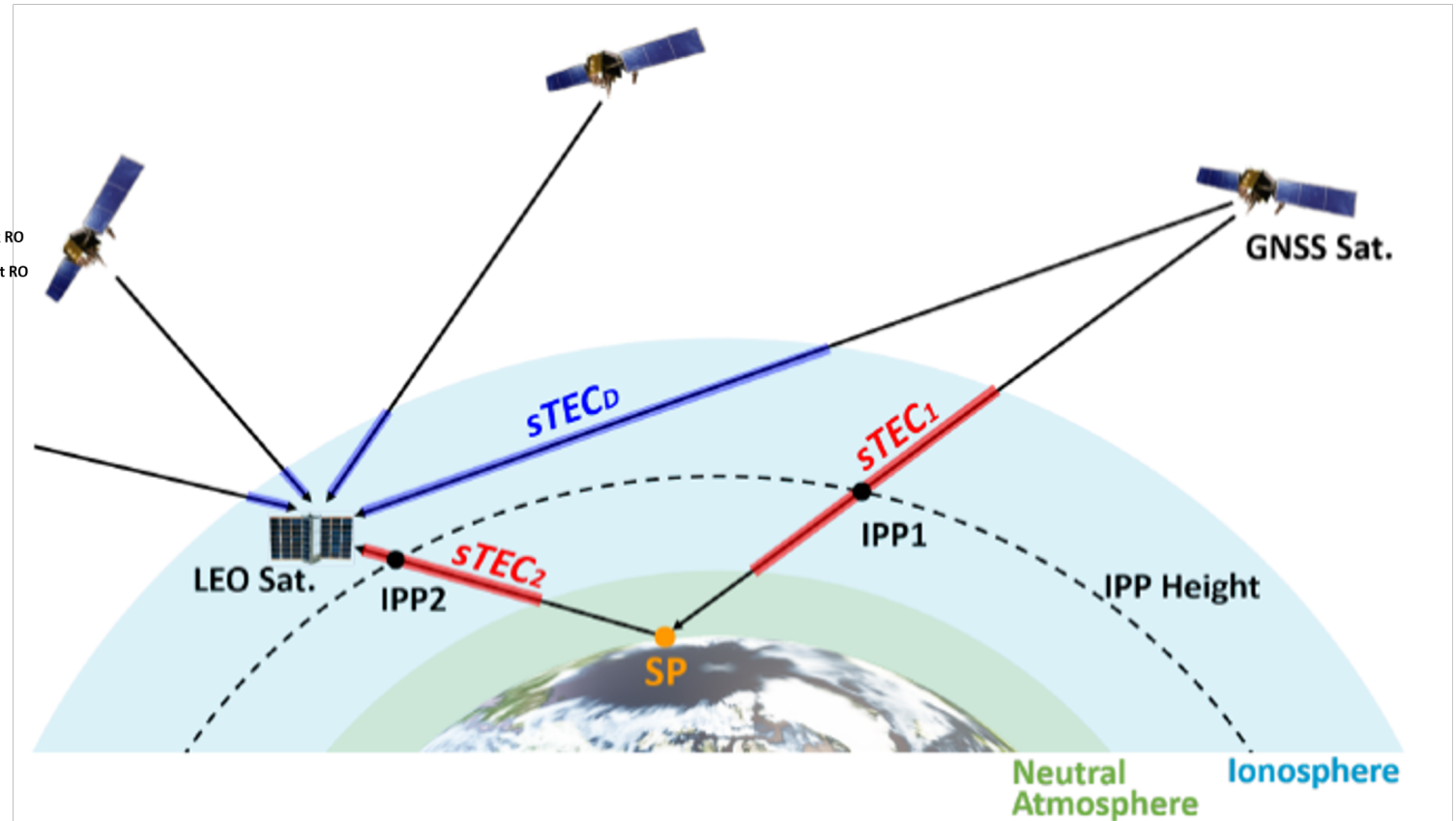
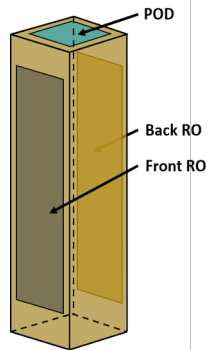
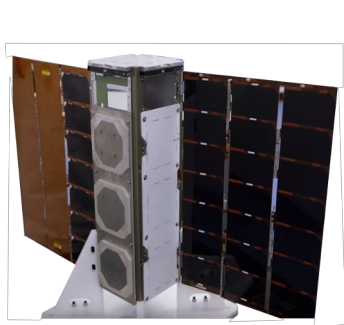
Oct. 2021



Sample Coherent Reflection Observation Distributions



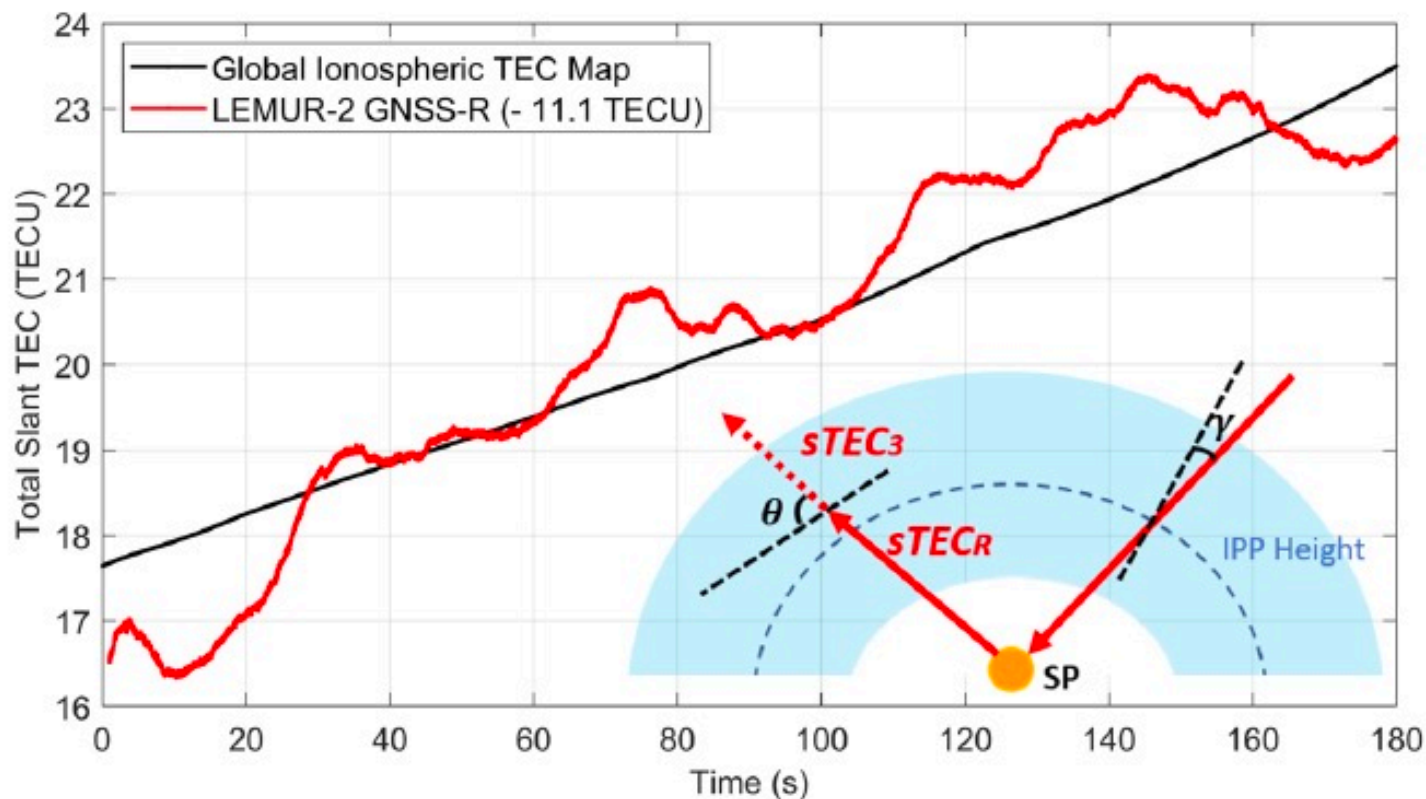
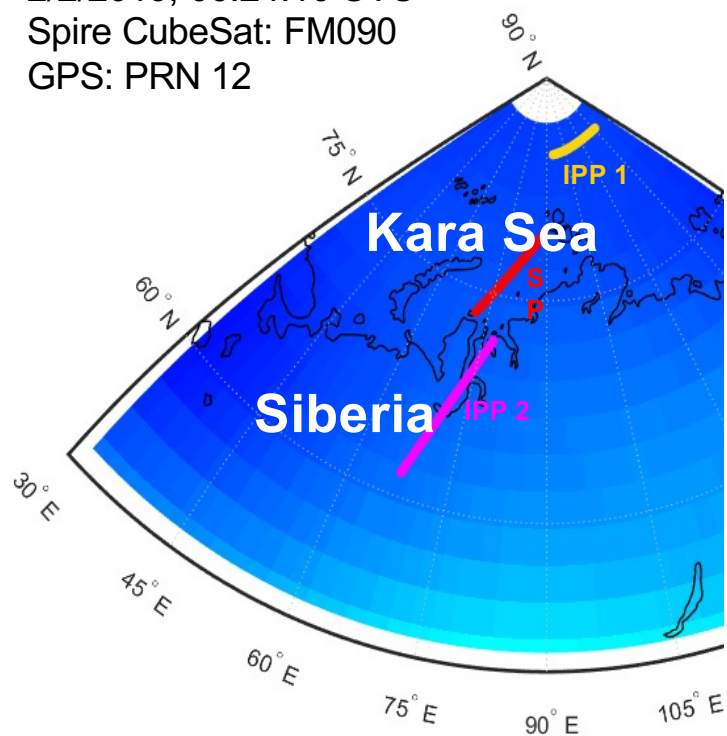
Spire Global CubeSat Dual-Frequency Measurements for Ionosphere Monitoring



Wang, Y., Y. J. Morton, "Ionospheric total electron content and disturbance observations from space borne coherent GNSS-R measurements," *IEEE Trans. Geosci. Remote Sensing*, DOI: 10.1109/TGRS.2021.3093328, 2021.

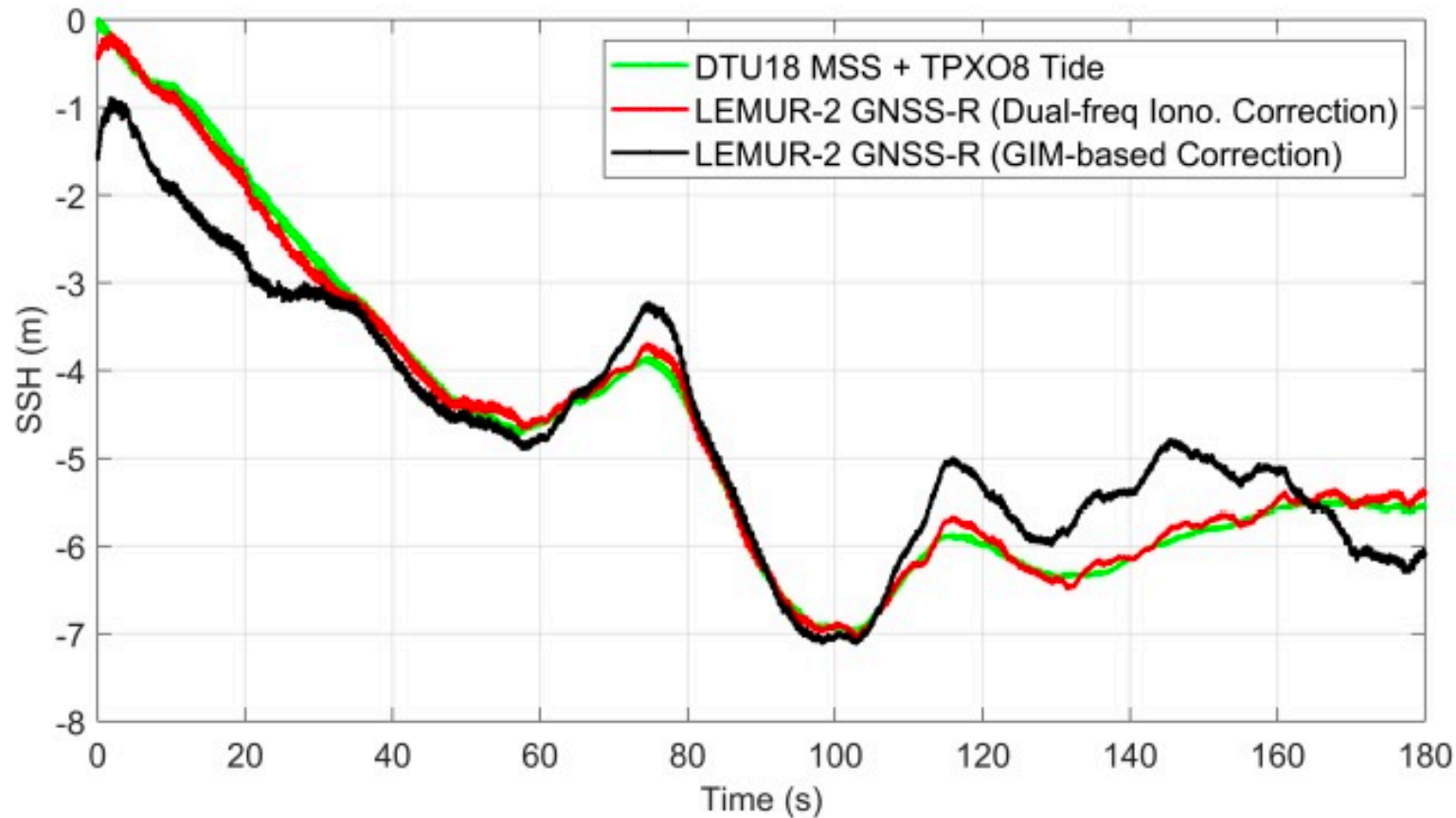
TEC Retrieval

2/2/2019, 06:24:16 UTC
Spire CubeSat: FM090
GPS: PRN 12



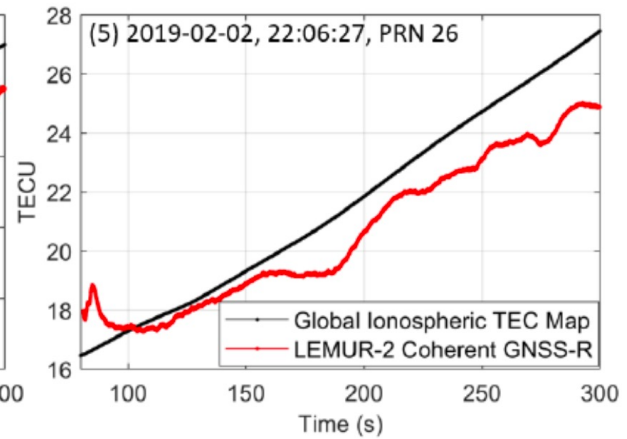
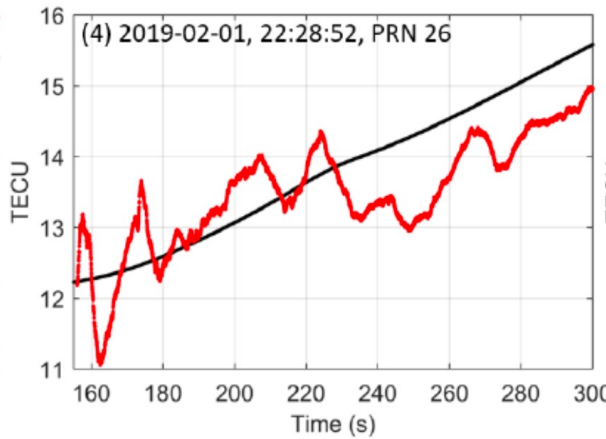
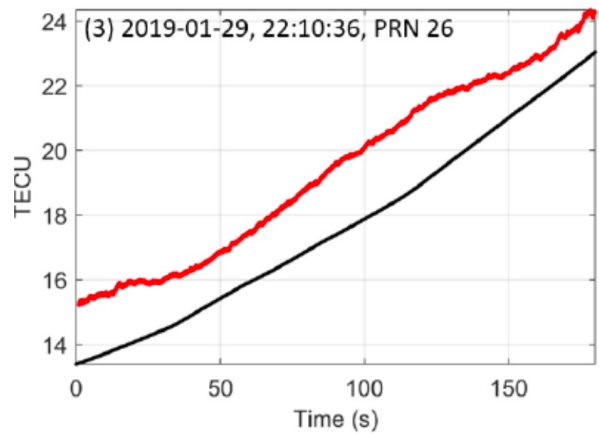
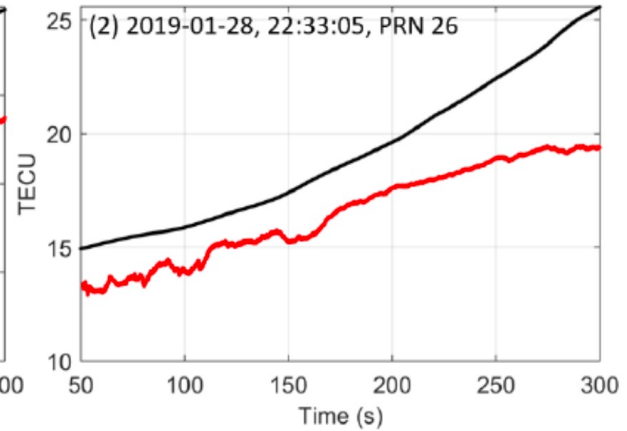
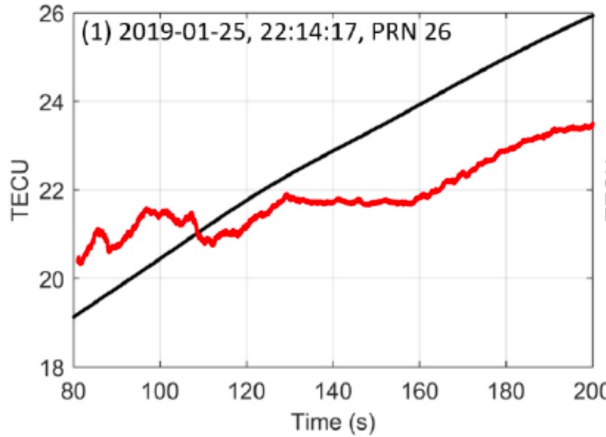
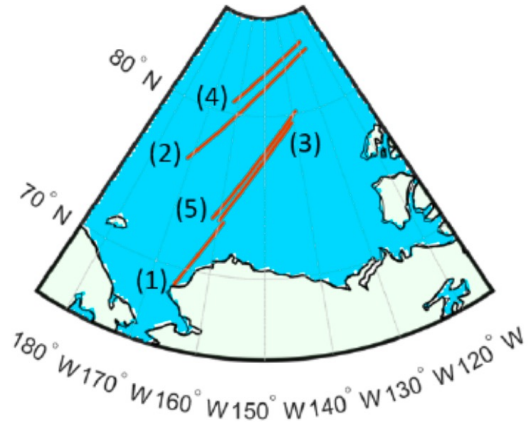
Wang, Y., Y. J. Morton, "Ionospheric total electron content and disturbance observations from space borne coherent GNSS-R measurements," *IEEE Trans. Geosci. Remote Sensing*, DOI: 10.1109/TGRS.2021.3093328, 2021.

Validation Based on Sea Surface Model: GNSS-R TEC vs. IGS GIM

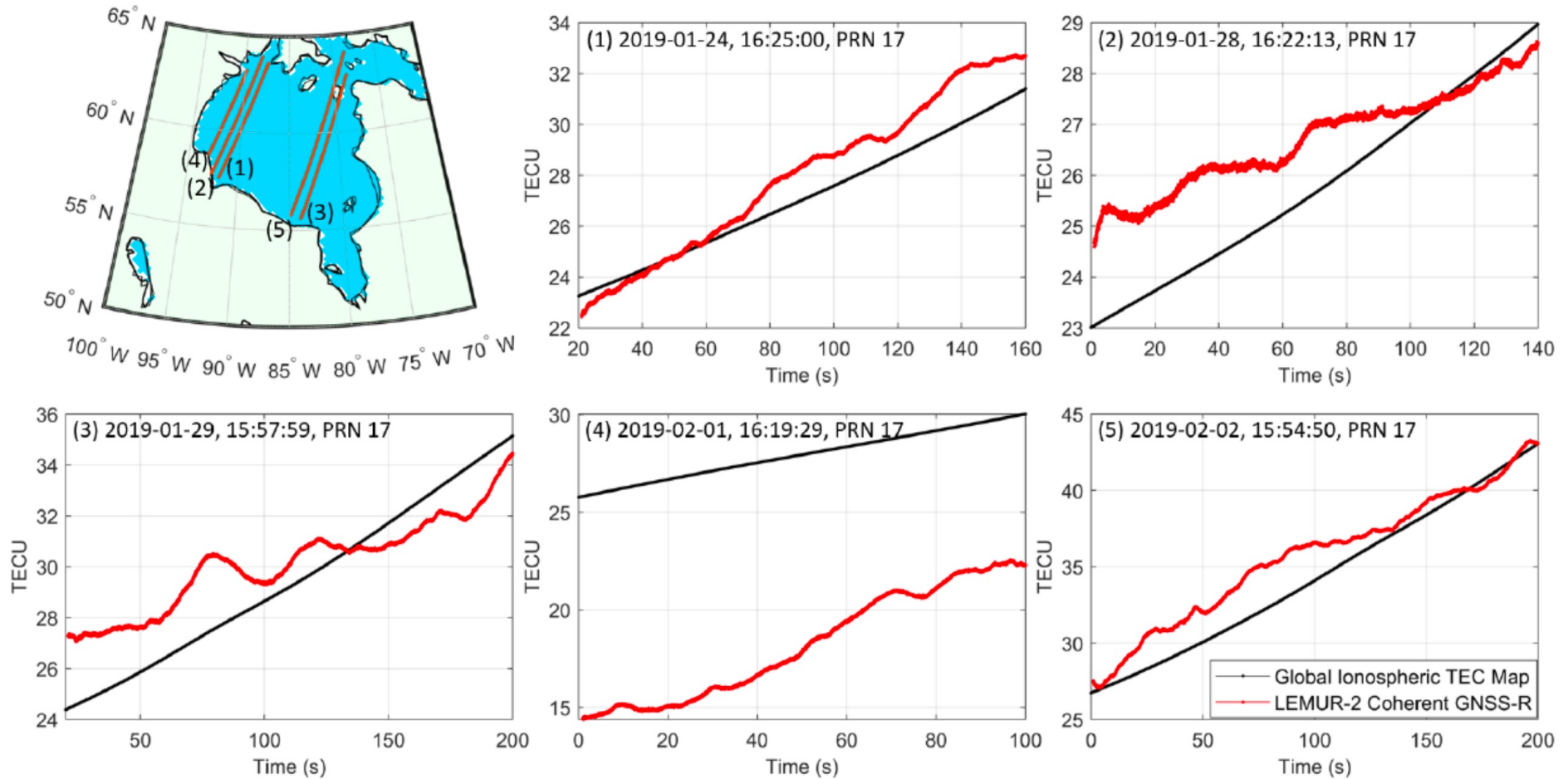


Wang, Y., Y. J. Morton, "Ionospheric total electron content and disturbance observations from space borne coherent GNSS-R measurements," *IEEE Trans. Geosci. Remote Sensing*, DOI: 10.1109/TGRS.2021.3093328, 2021.

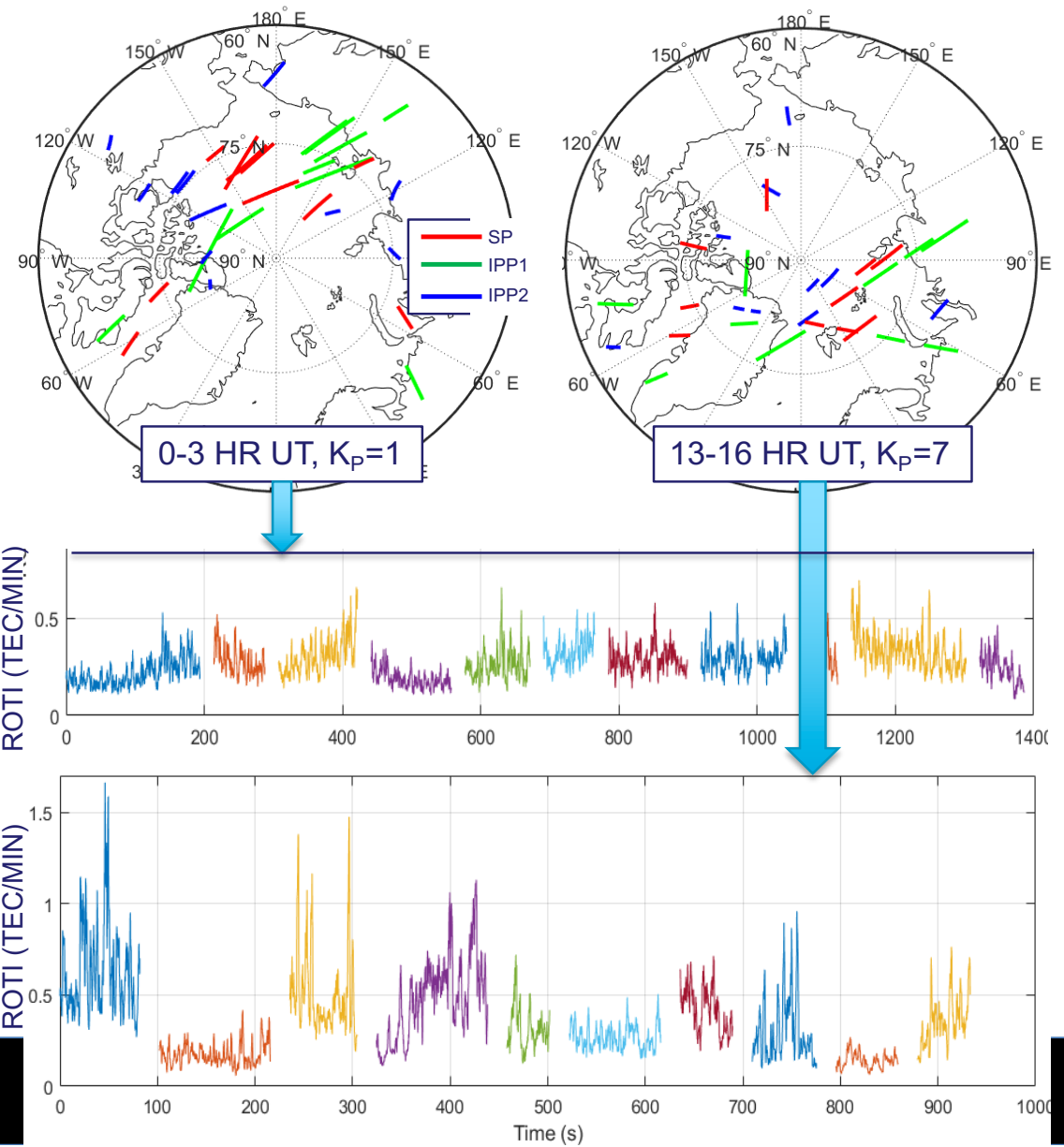
More Results Over Arctic Ocean



More Results Over Hudson Bay

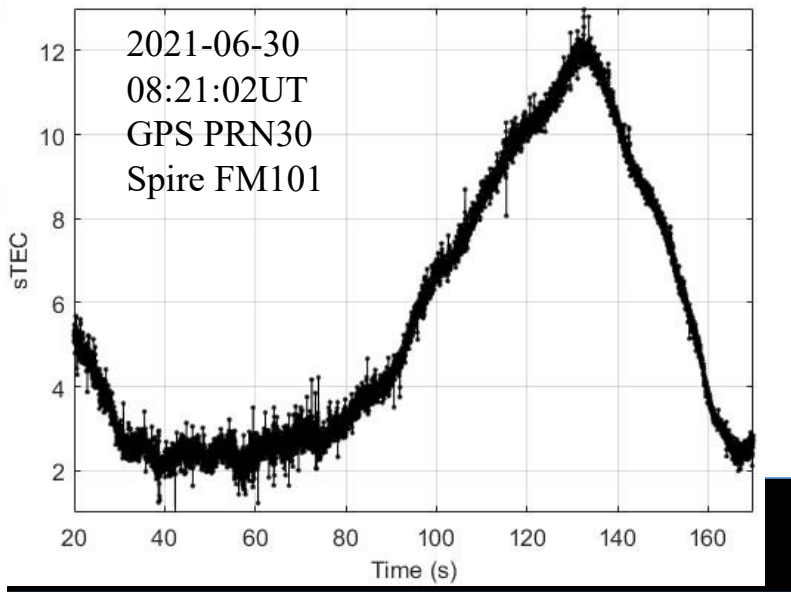
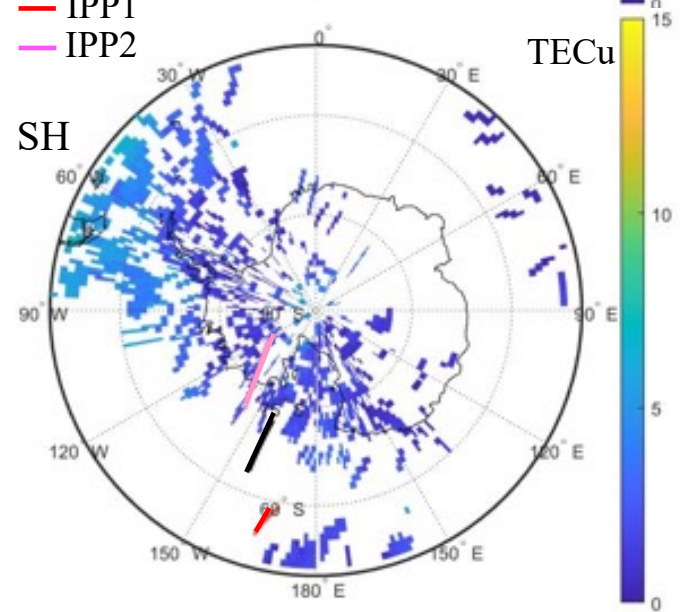
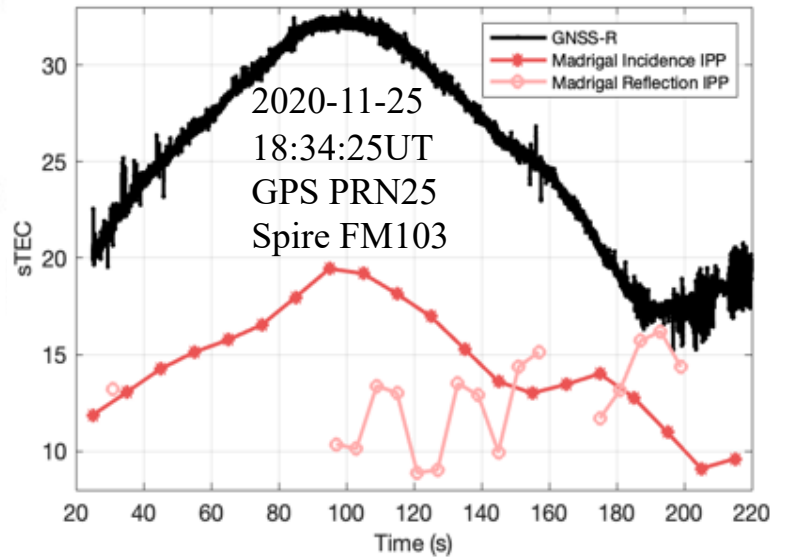
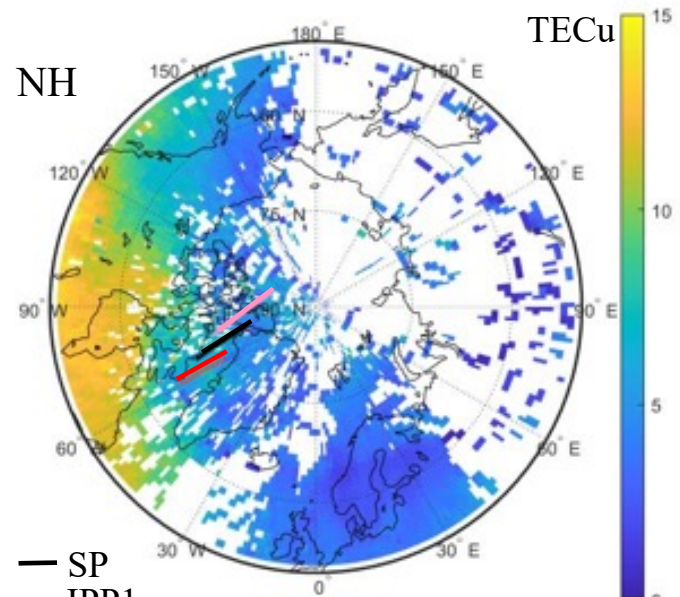


Ionospheric Disturbances Observation



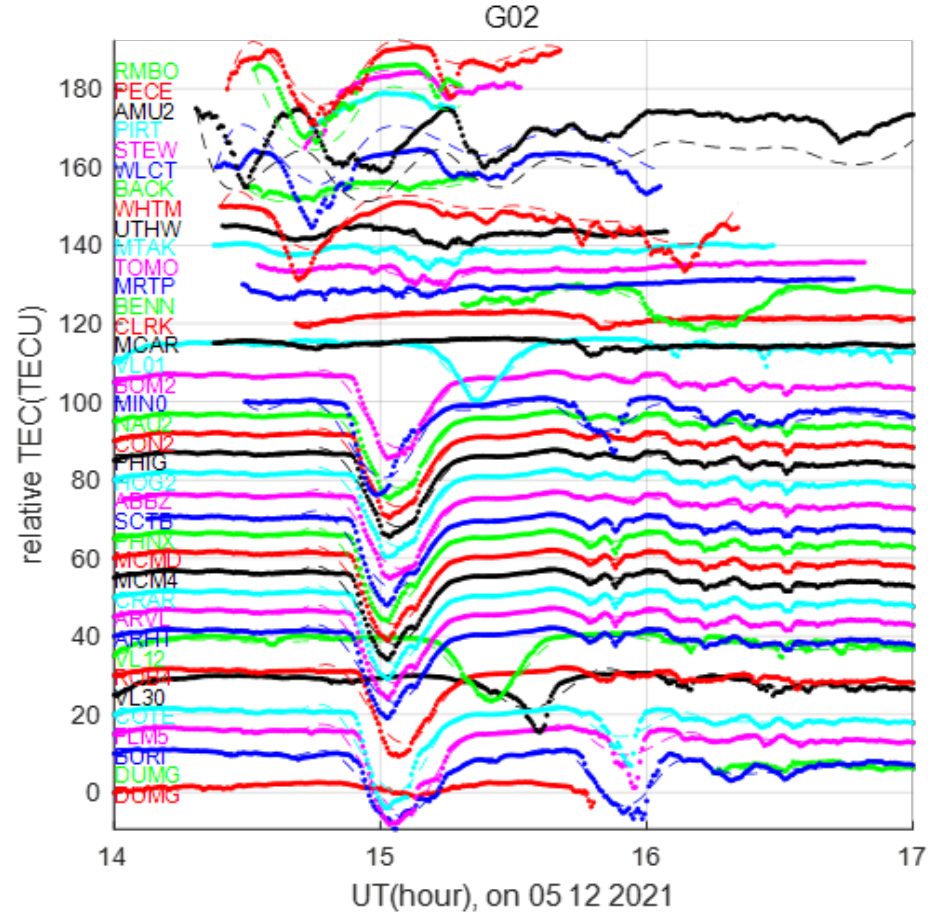
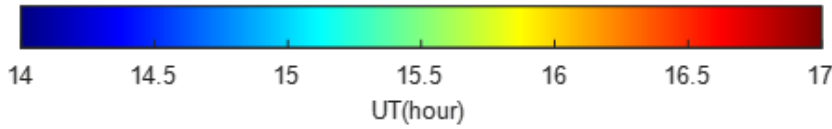
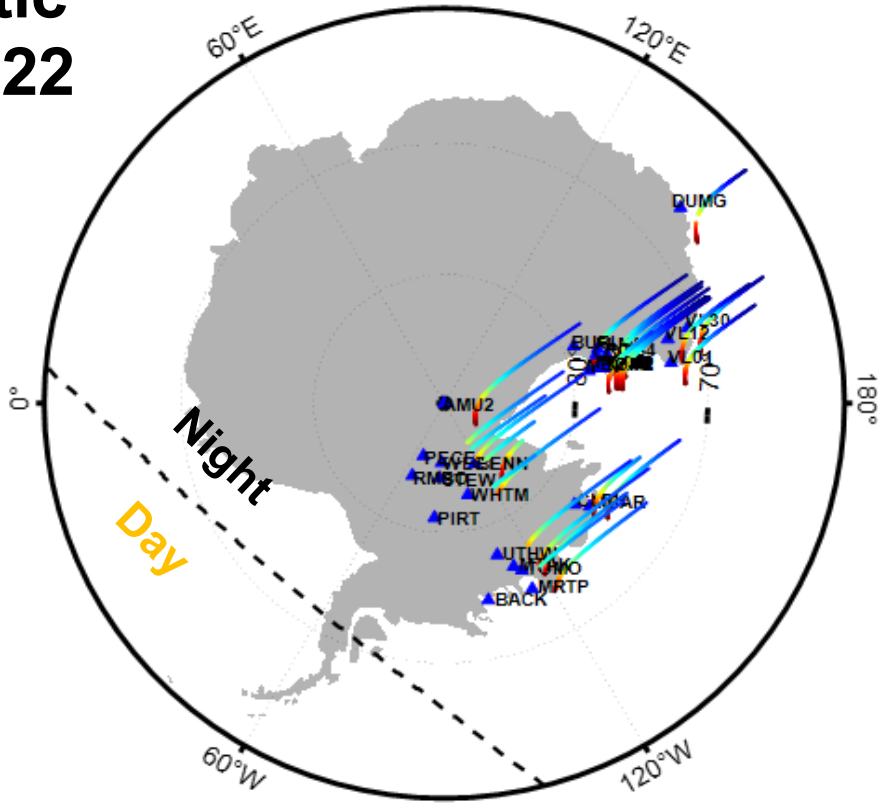
TEC Enhancement

Arctic 11/25/2011

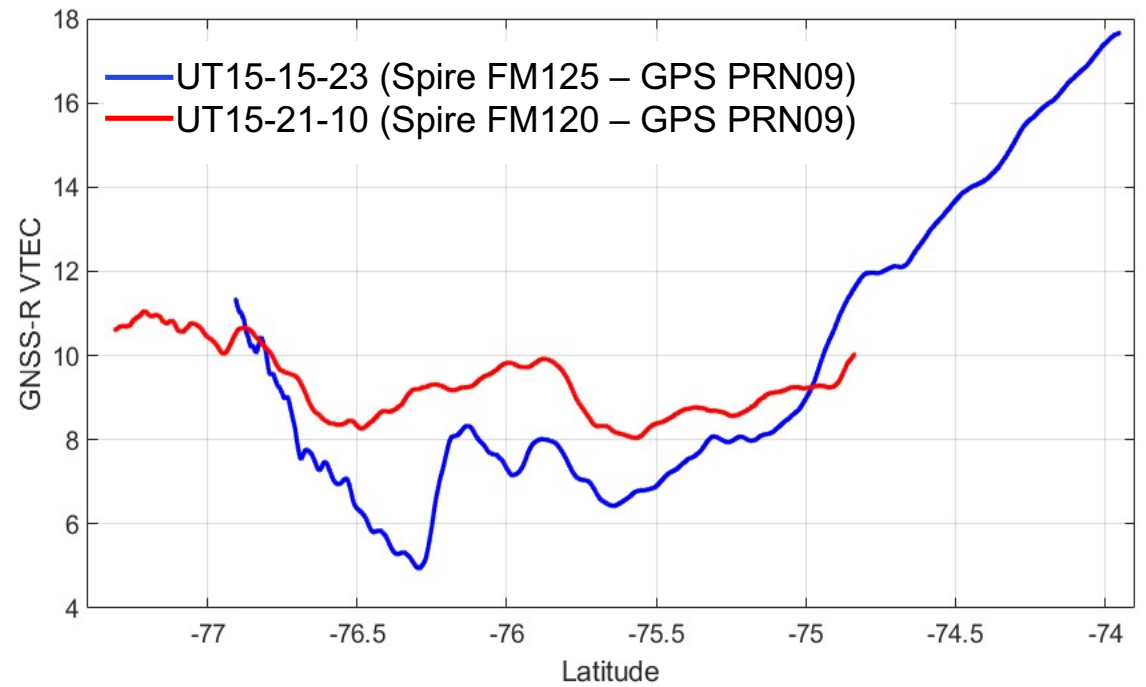
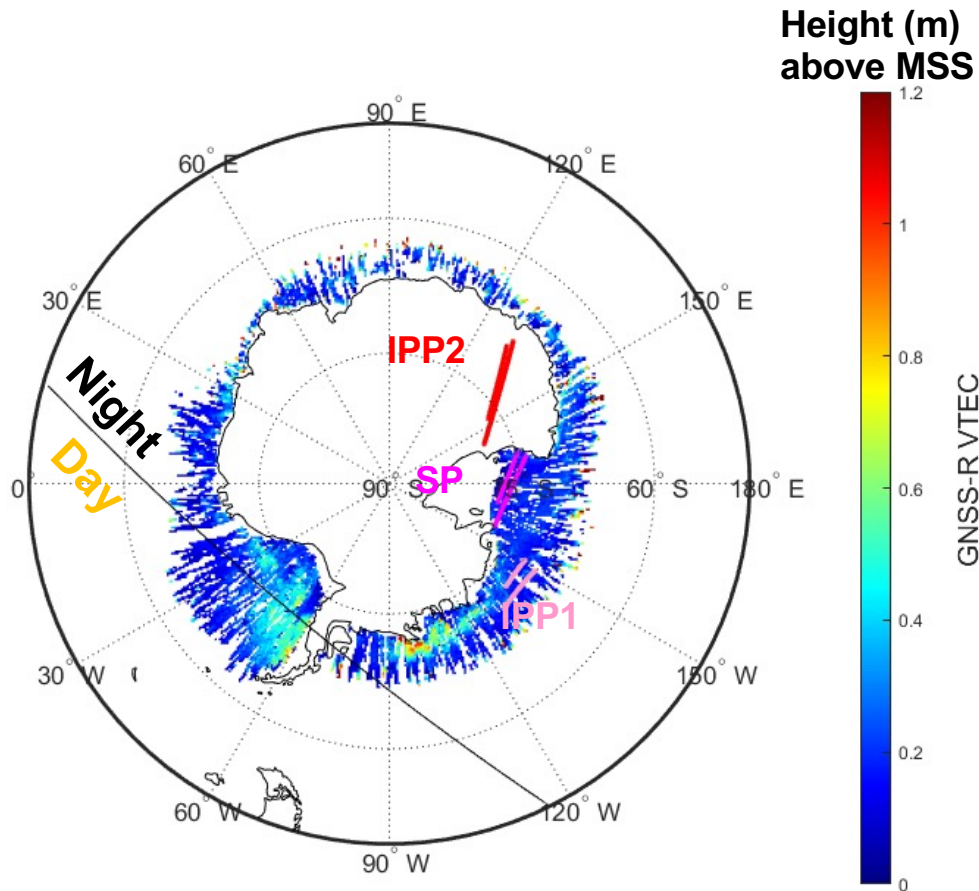


TEC Depletion Madrigal TEC Antarctic 5/12/2022

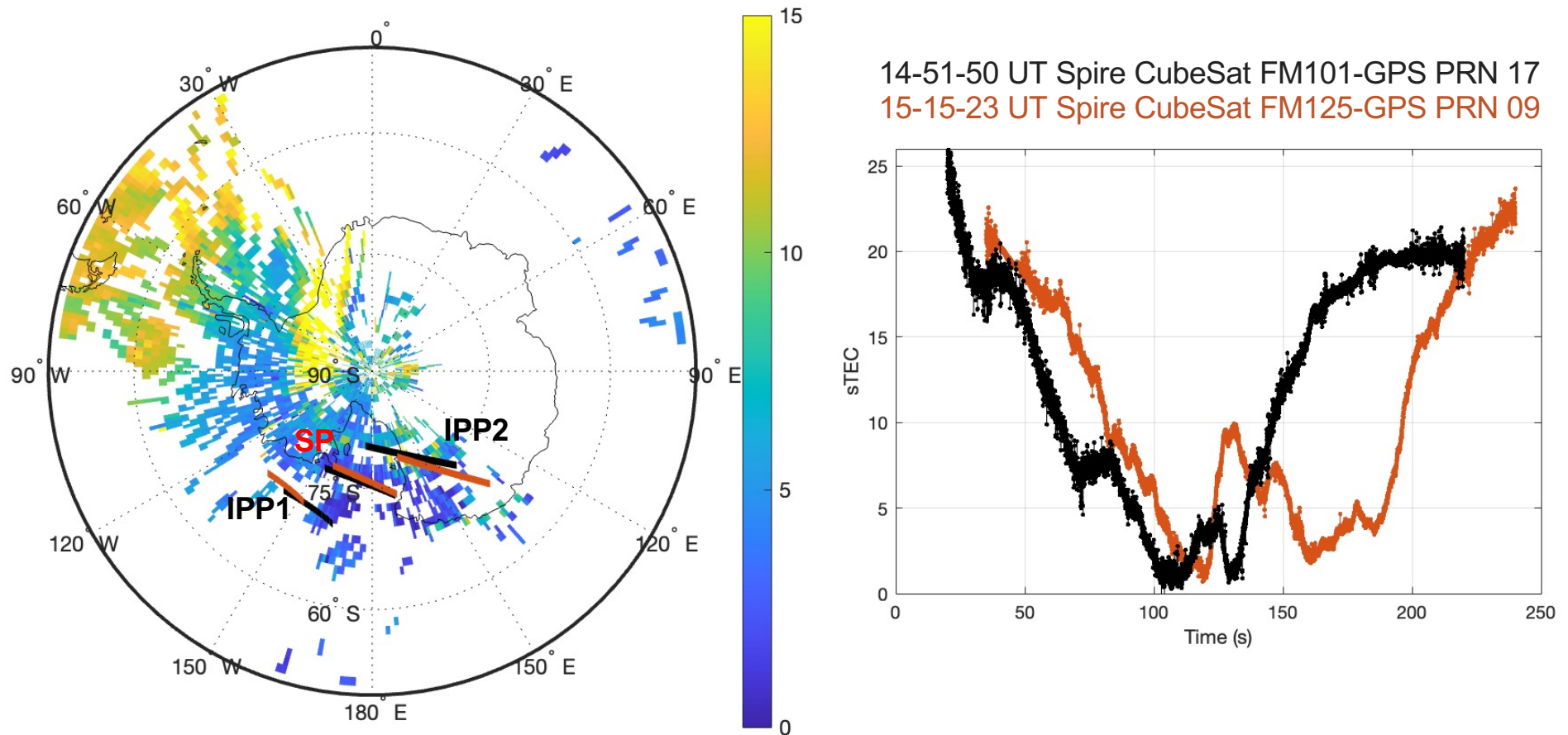
Ap	00-03h	03-06h	06-09h	09-12h	12-15h	15-18h	18-21h	21-00h
2021/05/12	42	1	1	4	4+	7	7-	2



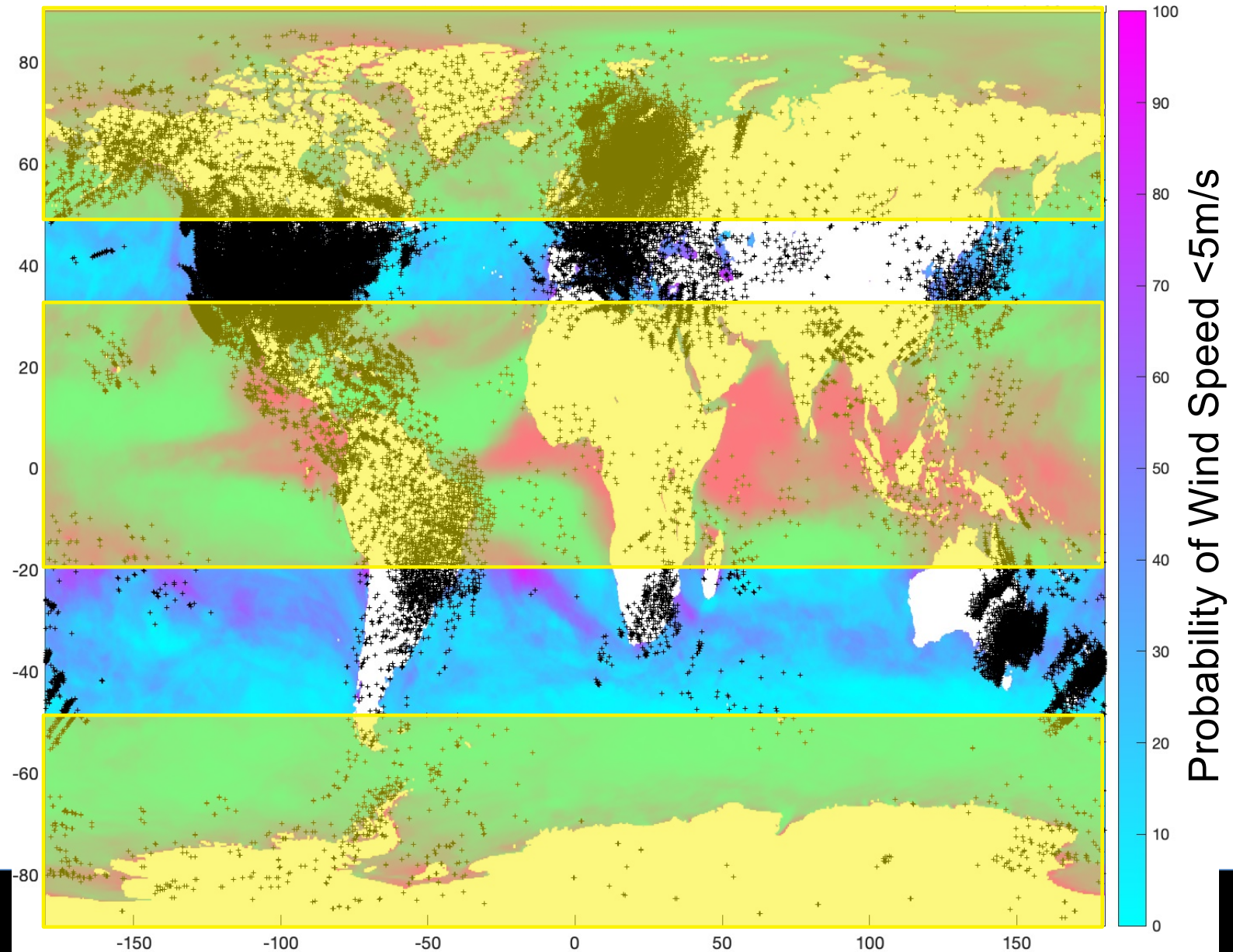
Spire CubeSat GNSS-R VTEC Observation: 5/12/2022



Spire CubeSat GNSS-R STEC Observation: 5/12/2022



**Regions with
High Probability
of Coherent
Reflections
+
Above
Inland Water
Bodies**



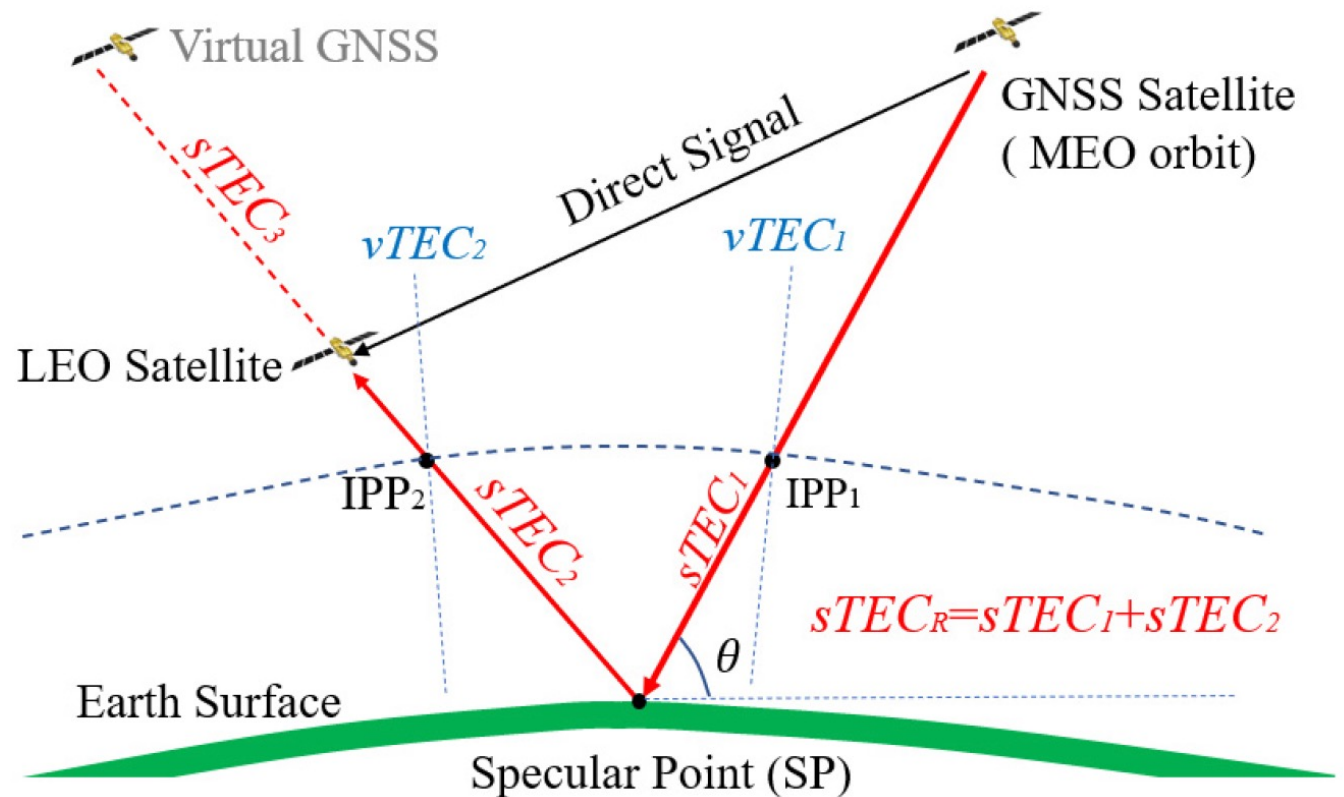
GNSS-R Ionosphere Monitoring Challenges

- Coherent reflection signal carrier tracking and cycle slip mitigation
- GNSS-R receiver hardware bias calibration
- Incidence and reflection ray contribution separation

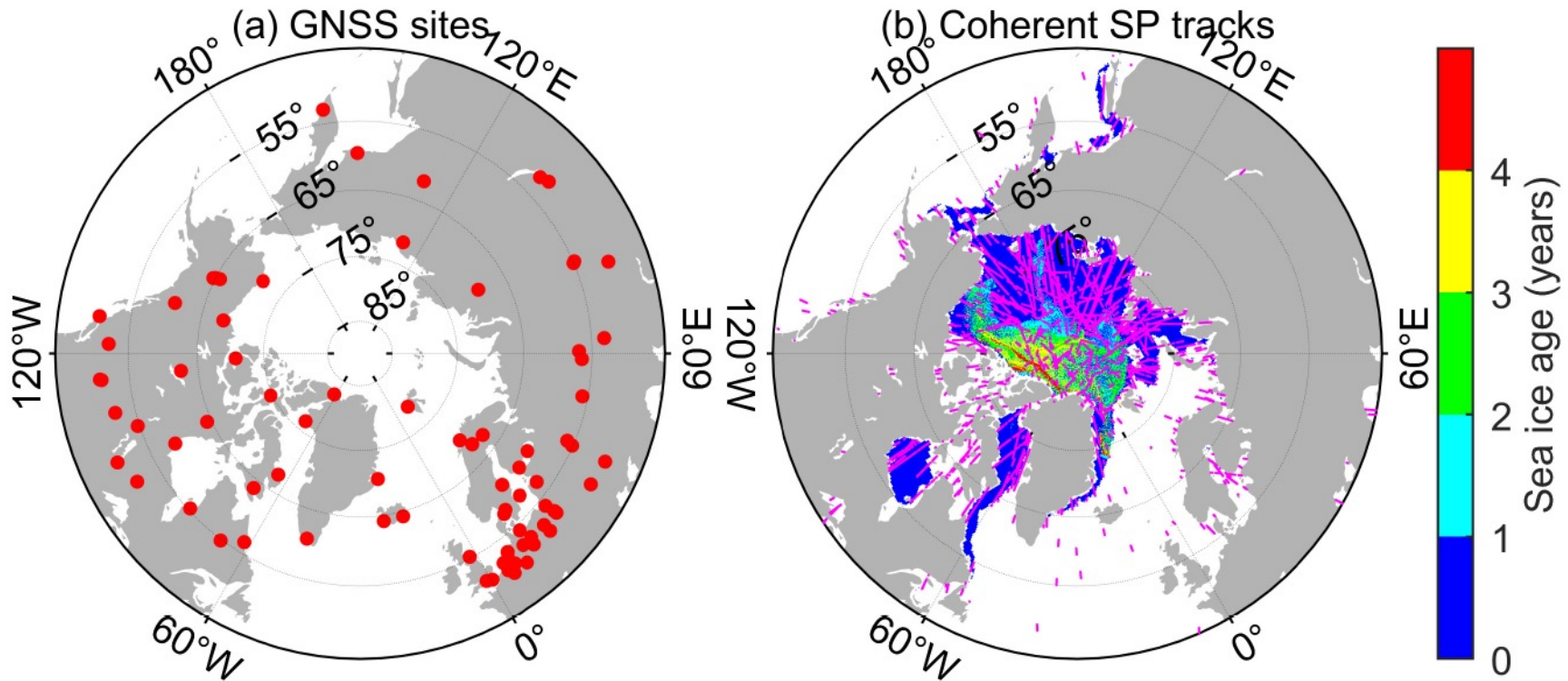


Separating TEC Contributions

$$(sTEC_R + sTEC_3) \cdot MF(\theta) = \sum_{i=i_1}^{i_2} \sum_{n=0}^{n_{\max}} \sum_{m=0}^n \tilde{P}_{nm}(\sin\phi_i) \cdot (a_{nm} \cos m \lambda_i + b_{nm} \sin m \lambda_i).$$

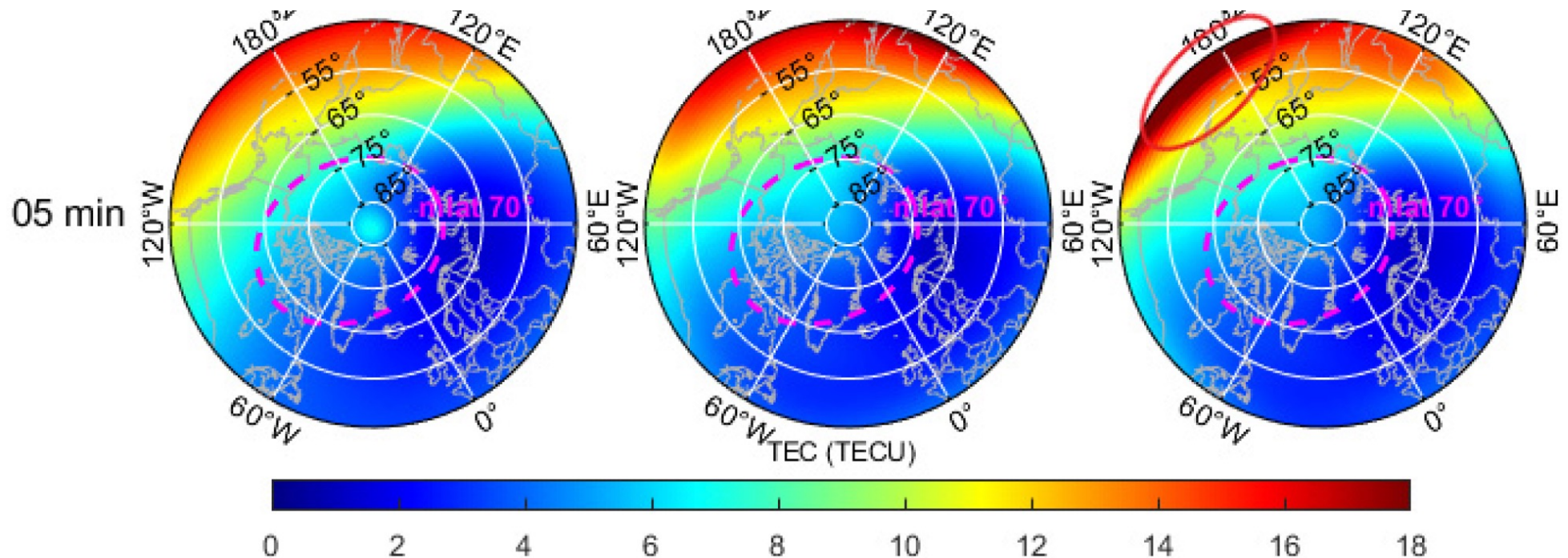


Simulation Studies



Liu, L., Y. J. Morton, Y. Wang, “Arctic TEC mapping using integrated LEO-based GNSS-R and ground-based GNSS observations: a simulation study,” *IEEE Trans. Geosci. Remote Sensing*, DOI: 10.1109/TGRS.2021.3138692, 2021.

TEC Map Construction: Using 5 Minutes Data



Liu, L., Y. J. Morton, Y. Wang, "Arctic TEC mapping using integrated LEO-based GNSS-R and ground-based GNSS observations: a simulation study," *IEEE Trans. Geosci. Remote Sensing*, DOI: 10.1109/TGRS.2021.3138692, 2021.

Conclusions

- GNSS-R has the potential to fill data gaps at critical regions (equatorial and high latitudes)
- GNSS-R offers nearly frozen-in time view of the ionosphere due to its rapid scan velocity
- There are challenges that need to be addressed. Potential methods under implementation.

Funding support:

NASA 80NSSC21K1553, 80NSSC20K1738, DARAP AWD-102938-G3

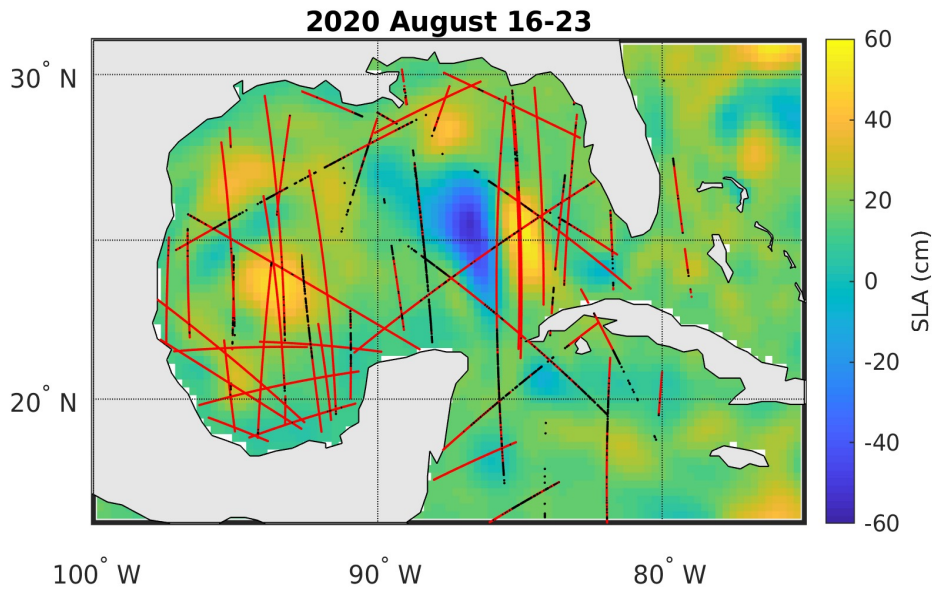
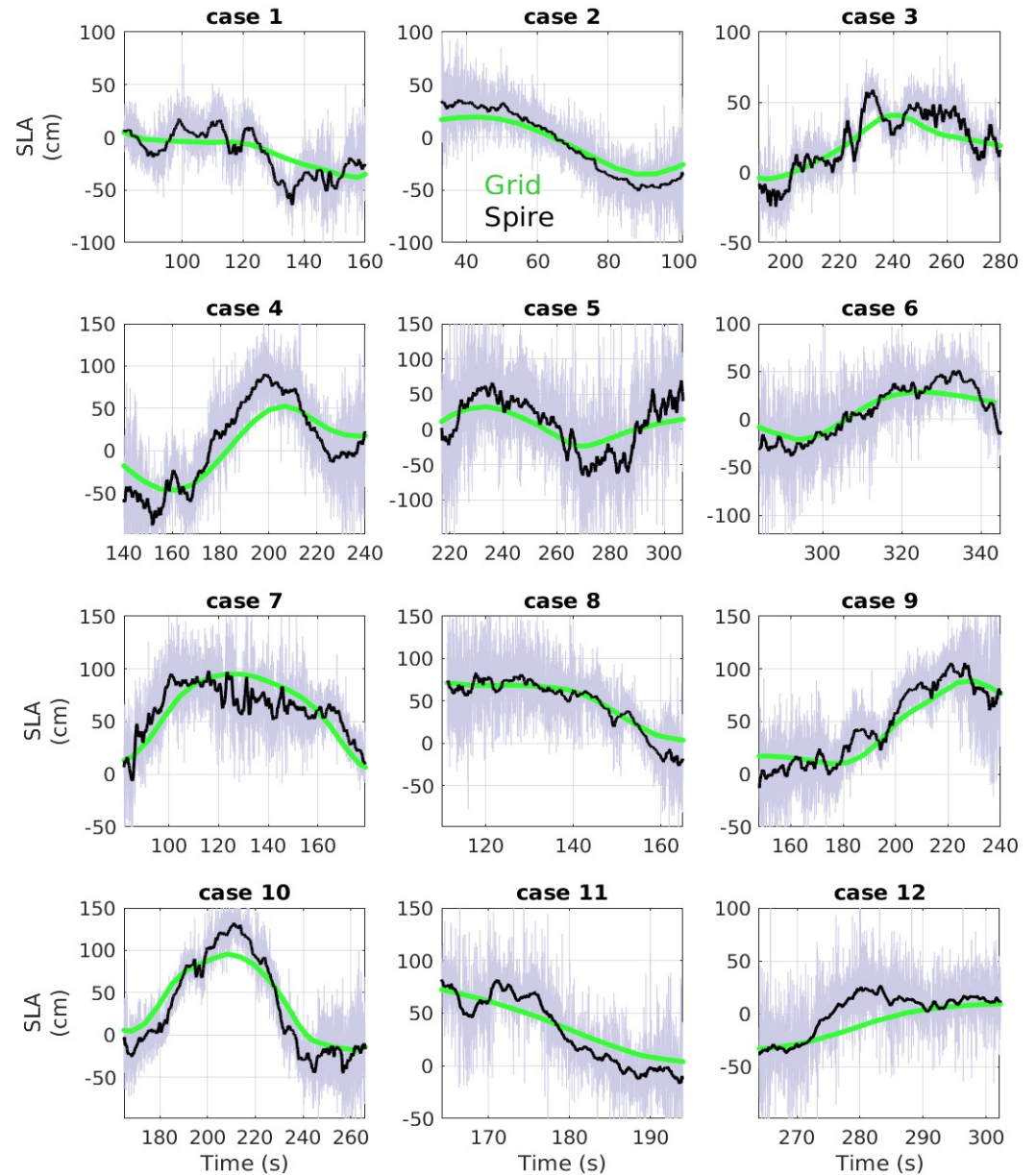


Backup Slides



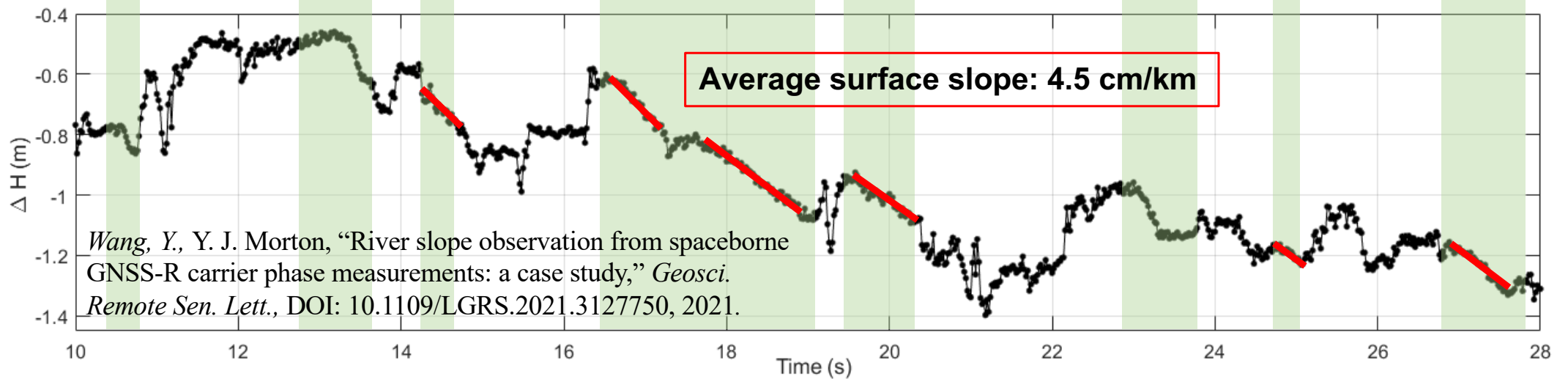
Gulf of Mexico

Sea Level Anomalies (SLA) at meter-level height and extending over 100km distance

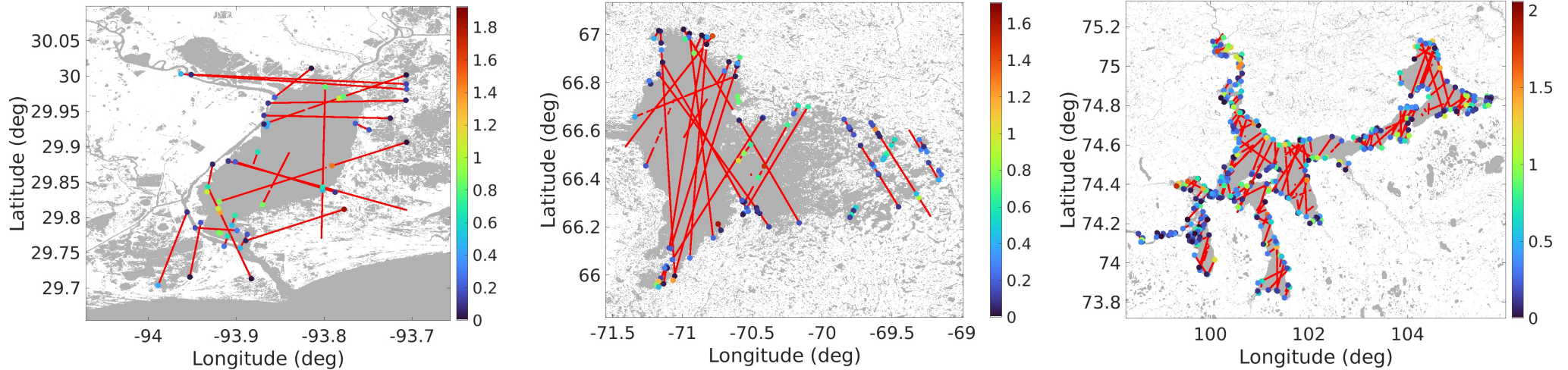


Roesler, C., Y. J. Morton, M. Scott, R. S. Nerem, "GNSS altimetry in the Gulf of Mexico based on Spire CubeSat carrier-phase data," *Proc. IEEE GNSS+R Special Meeting on GNSS+R*, DOI: [10.1109/GNSSR53802.2021.9617729](https://doi.org/10.1109/GNSSR53802.2021.9617729), 2021.

River Surface Slope Retrieval



Masking Inland Water Body Boundary

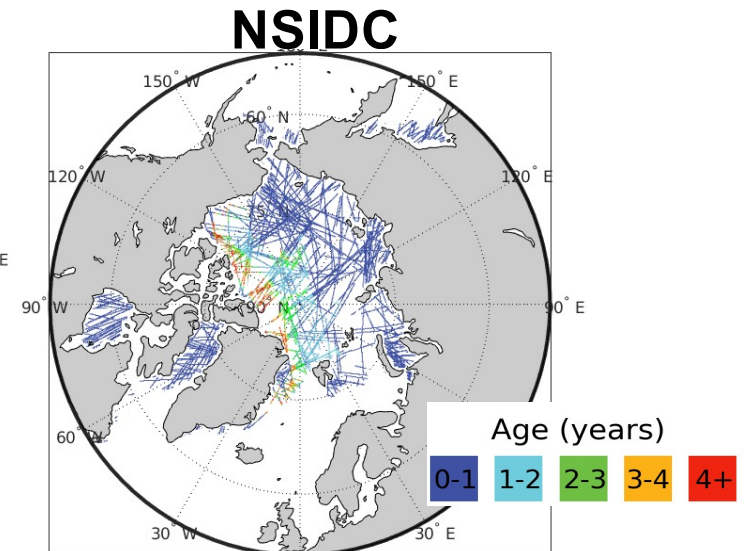
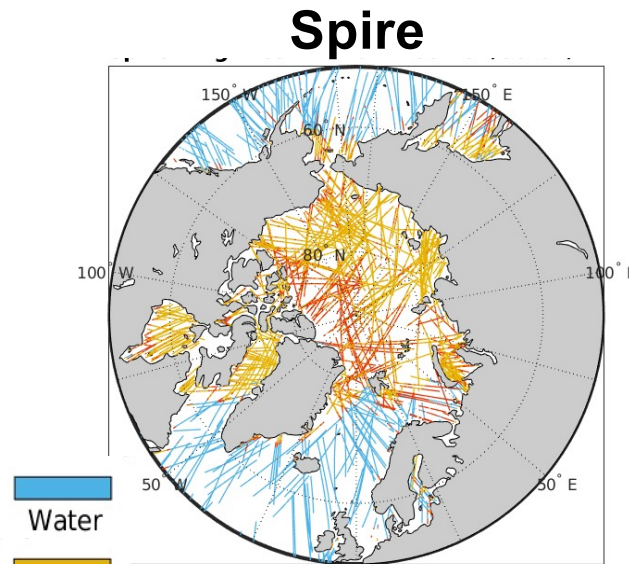


Zhang, J., Y. J. Morton, Y. Wang, and C. Roesler, “Delineating lake boundaries by using raw GNSS-R measurements” Presented at the CYGNSS Science Team Meeting, March 9, 2022.

Comparison: Spire vs. NSIDC Sea Ice Age Data

4/8 – 4/14, 2020

NH



SH

